IMSc/98/06/26

One pion events by atmospheric neutrinos: A three flavor analysis

K. R. S. Balaji, G. Rajasekaran

Institute of Mathematical Sciences, Chennai 600 113, India.

S. Uma Sankar

Department of Physics, I.I.T. , Powai, Mumbai 400076, India

(February 1, 2008)

Abstract

We study the one-pion events produced via neutral current (NC) and charged current (CC) interactions by the atmospheric neutrinos. We analyze the ratios of these events in the framework of oscillations between three neutrino flavors. The ratios of the CC events induced by ν_e to that of the NC events and a similar ratio defined with ν_μ help us in distinguishing the different regions of the neutrino parameter space.

PACS numbers:14.60.pq, 13.15.+g, 95.85.Ry

I. INTRODUCTION

It has been more than a decade since the atmospheric neutrino anomaly has been observed by the water Cerenkov detectors IMB [1] and Kamiokande [2,3]. Eventhough conventional detectors Frejus [4] and NUSEX [5] have not observed this effect, a recent experiment SOUDAN-II did indeed see a deficit [6]. Recent results from Superkamiokande confirmed the earlier results including the zenith angle dependence of the deficit in the multi-GeV data [7]. The results of all these experiments are presented in the form of the double ratio

$$R = \frac{\left(\frac{N_{\nu_\mu}}{N_{\nu_e}}\right)_{obs}}{\left(\frac{N_{\nu_\mu}}{N_{\nu_e}}\right)_{MC}} = \frac{r_{obs}}{r_{MC}}. \tag{1}$$

The measured value of R for Kamiokande is $0.60^{+0.07}_{-0.06} \pm 0.05$ for sub-GeV data (E $<$ 1.33 GeV) and $0.57^{+0.08}_{-0.07} \pm 0.07$ for the multi-GeV data (E $>$ 1.33 GeV) whereas that of Superkamiokande is $0.61 \pm 0.06 \pm 0.05$ for sub-GeV and $0.67 \pm 0.06 \pm 0.08$ for the multi-GeV data. The reason for presenting the result in the form of the double ratio is that the theoretical calculations of ν_μ and ν_e fluxes are subject to large uncertainties of the order of 30% [8,9]. Hence a comparison of measured neutrino flux with the calculated one (either for ν_μ or for ν_e) is not particularly useful. However, the uncertainties in the ratios of the calculated fluxes are much smaller (less than 10%). Hence a comparison of the measured ratio of ν_μ flux to ν_e flux to the calculated ratio will yield meaningful information on neutrino properties.

Neutrino oscillations provide a natural explanation for both the overall deficit and the zenith angle dependence [10,11]. Kamiokande analyzed their data in terms of two flavor oscillations between $\nu_\mu \leftrightarrow \nu_e$ and $\nu_\mu \leftrightarrow \nu_\tau$. In both cases they found allowed regions of parameter space, with the mass-squared difference around $\Delta m^2 \simeq 0.02\ eV^2$ and the mixing angle near its maximal value of $\pi/4$ [3]. The analysis of Superkamiokande yields roughly the same mixing angle but a lower value of $\Delta m^2 \simeq 0.001\ eV^2$ [7,12]. Since both $\nu_\mu \leftrightarrow \nu_e$ and $\nu_\mu \leftrightarrow \nu_\tau$ oscillations give equally good allowed regions, one must look for ways of distinguishing which type of oscillations are the cause of the atmospheric neutrino anomaly.

Recently Vissani and Smirnov (VS) [13] proposed that the single pion events in the energy range 0.5 GeV - 1.5 GeV can be used to distinguish between different types of oscillations. Such events induced by neutral current (NC) contain a π^0 whereas the events induced by charged current (CC) contain a π^+ or π^-. The $\pi^\pm$ are detected as sharp rings, whereas the π^0 decays into two photons which are detected as two diffuse rings. Kamiokande has already observed such π^0's in their detector by considering all events with two diffuse rings and by selecting those events with invariant mass in the range 90 MeV - 180 MeV [14]. The CC events due to ν_e contain an $e^\mp$ in addition to a $\pi^\pm$ and those due to ν_μ contain a $\mu^\mp$. Thus one can distinguish an NC event (two difuse rings with the invariant mass of the rings around m_π) from a ν_e CC event (one diffuse ring due to $e^\mp$ and one sharp ring due to $\pi^\pm$) and from a ν_μ CC event (two sharp rings from $\mu^\mp$ and $\pi^\pm$). The two ratios, NC events to ν_e CC events and NC events to ν_μ CC events, are free from the uncertainties of the theoretical flux calculations. The ratio of the cross sections of the NC to CC events in single pion production were measured previously [15] and the uncertainties in them are about 15%. Hence a measurement of the above ratios can help in distinguishing the different types of oscillations which are currently relevant for atmospheric neutrino anomaly.

In this paper we analyze the atmospheric neutrino problem in the framework of oscillations between three active flavors. We will assume that one of the masses is much greater than the other two. We fix the smaller of the mass-squared differences using the solar neutrino data [16,17]. Then the larger mass-squared difference and two of the mixing angles are relevant for the atmospheric neutrino problem [18]. The double ratio R defined in equation(1), along with the zenith angle dependent multi-GeV data, was analyzed in this framework previously [19,20]. Here we analyze the ratio of CC to NC events for one-pion production in the framework of three active neutrino oscillations and see how they can distinguish between different regions of parameter space. The NC event rate is unaffected by the oscillations while the CC event rate is affected by the oscillations and hence depend on the neutrino parameters. In section II we give the basic theory for the calculation of the one-pion event rates in the three-flavor oscillation scenario. This is followed by the discus-

sion of the experimentally measurable quantities in section III and a summary is given in section IV.

II. THEORY

In a three flavor scheme, the weak eigenstates ν_α are related to the mass eigenstates ν_i through a 3×3 unitary matrix U as

$$\nu_\alpha = \sum_i U_{\alpha i}\nu_i. \tag{2}$$

U can be written as

$$U = U^{23}(\psi) \times U^{phase} \times U^{13}(\phi) \times U^{12}(\omega), \tag{3}$$

where, $U^{ij}(\theta_{ij})$ is the two flavor mixing matrix between the ith and jth mass eigenstates with mixing angles θ_{ij}. We assume CP invariance and set $U^{phase} = I$. For the neutrinos that propagate through matter, the CC interaction between ν_e and e induces an effective mass term for the ν_e which is of the form $A = 2\sqrt{2}G_F N_e E$, where N_e is the electron number density and E is neutrino energy. Single-pion production maximally occurs for neutrinos within the energy range of 0.5 GeV - 1.5 GeV. For this energy region, matter effects in the earth can be neglected since $A < 10^{-4}\ eV^2$ and $\delta_{31} \simeq 10^{-3}\ eV^2$, as given by Superkamiokande analysis [7,12]. This choice for δ_{31} is consistent with the mass heirarchy assumption under which both the atmospheric and solar neutrino anamalies can be explained. Hence, here we have the simple case of vacuum oscillations. The vacuum oscillation probability $P_{\alpha\beta}$ for a neutrino with a flavor α to oscillate in to a flavor β can be given by

$$P_{\alpha\beta} = U^2_{\alpha1}U^2_{\beta1} + U^2_{\alpha2}U^2_{\beta2} + U^2_{\alpha3}U^2_{\beta3} + 2U_{\alpha1}U_{\alpha2}U_{\beta1}U_{\beta2}cos\left(\frac{2.53x\delta_{21}}{E}\right) + 2U_{\alpha1}U_{\alpha3}U_{\beta1}U_{\beta3}cos\left(\frac{2.53x\delta_{31}}{E}\right) + 2U_{\alpha3}U_{\alpha2}U_{\beta3}U_{\beta2}cos\left(\frac{2.53x\delta_{32}}{E}\right). \tag{4}$$

Here, E is the energy of the neutrino in GeV, x is the distance travelled by the neutrino in kilometers and δ_{ij} is $m_i^2 - m_j^2$ in eV^2. We assume the mass heirarchy ($\delta_{21} \ll \delta_{32} \simeq$

δ_{31}) as suggested by the variuos analyses of the solar and atmospheric neutrino problems [3,19,20,16–18,21] and take $\delta_{21} \simeq 0$, which allows us to put the oscillating term involving δ_{21} as unity. So we get

$$P_{\alpha\beta} = (U_{\alpha1}U_{\beta1} + U_{\alpha2}U_{\beta2})^2 + (U_{\alpha3}U_{\beta3})^2 + 2(U_{\alpha1}U_{\beta1} + U_{\alpha2}U_{\beta2})U_{\alpha3}U_{\beta3}cos\left(\frac{2.53\delta_{31}x}{E}\right). \quad (5)$$

Since we are considering vacuum oscillations with CP invariance, the oscillation probability for antineutrinos is the same as that for neutrinos.

The various one-pion events arising from NC and CC interaction are listed below:

$$\nu_l N \rightarrow \nu_l \pi^0 N, \qquad l = e, \mu, \tau, \quad (6)$$

$$\nu_l N \rightarrow l \pi^0 N', \qquad l = e, \mu, \quad (7)$$

$$\nu_e N \rightarrow e^- \pi^+ N, \quad (8)$$

$$\nu_\mu N \rightarrow \mu^- \pi^+ N, \quad (9)$$

where, N and N' refer to the nucleons. As we are dealing with sub-GeV neutrinos, ν_τ do not excite CC processes. For every neutrino reaction, we consider the corresponding anti-neutrino reaction also.

It is difficult to calculate the zenith-angle dependent fluxes for sub-GeV neutrinos [8,9] and further the scattering angle of the final state charged lepton for neutrinos in the sub-GeV range can be as large as 60^o and thus directionality is lost in the detection process. Moreover, the event rates for the one-pion events that we consider are not very large. Hence we will not consider zenith angle dependence and will average over the zenith angle, or equivalently, over x, the distance travelled by the neutrinos in its allowed range (20 Km -13000 Km).

The NC rate N^{NC} (with π^0 as the detectable final state particle) is given by

$$N^{NC} = \int_{0.5GeV}^{1.5GeV} dE \left[\frac{d\Phi_e(E)}{dE} + \frac{d\Phi_\mu(E)}{dE}\right] \sigma^{NC}(E)\ \epsilon_{\pi^0}, \quad (10)$$

where, σ^{NC} is the scattering cross section for the reaction of Eq. (6) and ϵ_{π^0} is the π^0 detection efficiency which is 0.77 for the energy range of interest. N^{NC} being flavor blind

remains unaffected by oscillations. The CC rates arising from processes (7-9) can be written as

$$N^{CC}_{\mu^-\pi^+} = \frac{1}{12980}\int_{0.5GeV}^{1.5GeV} dE \int_{20Km}^{13000Km} dx \left[\frac{d\Phi_\mu(E)}{dE}P_{\mu\mu}(E,x) + \frac{d\Phi_e(E)}{dE}P_{e\mu}(E,x)\right] \sigma^{\pi^+}_{\mu^-}(E)\epsilon_{\pi^+}\epsilon_{\mu^-}, \quad (11)$$

$$N^{CC}_{e^-\pi^+} = \frac{1}{12980}\int_{0.5GeV}^{1.5GeV} dE \int_{20Km}^{13000Km} dx \left[\frac{d\Phi_e(E)}{dE}P_{ee}(E,x) + \frac{d\Phi_\mu}{dE}(E)P_{\mu e}(E,x)\right] \sigma^{\pi^+}_{e^-}(E)\epsilon_{\pi^+}\ \epsilon_{e^-}. \quad (12)$$

$$N^{CC}_{\mu^-\pi^0} = \frac{1}{12980}\int_{0.5GeV}^{1.5GeV} dE \int_{20Km}^{13000Km} dx \left[\frac{d\Phi_\mu(E)}{dE}P_{\mu\mu}(E,x) + \frac{d\Phi_e(E)}{dE}P_{e\mu}(E,x)\right] \sigma^{\pi^0}_{\mu^-}(E)\epsilon_{\pi^0}\epsilon_{\mu^-}, \quad (13)$$

$$N^{CC}_{e^-\pi^0} = \frac{1}{12980}\int_{0.5GeV}^{1.5GeV} dE \int_{20Km}^{13000Km} dx \left[\frac{d\Phi_e(E)}{dE}P_{ee}(E,x) + \frac{d\Phi_\mu}{dE}(E)P_{\mu e}(E,x)\right] \sigma^{\pi^0}_{e^-}(E)\epsilon_{\pi^0}\ \epsilon_{e^-}. \quad (14)$$

In each of the above equations the events due to antineutrinos are added to those due to neutrinos. Here, ϵ_{e^+}, ϵ_{μ^+} and ϵ_{π^-} are the electron, muon and the charged pion detection efficiencies respectively, which in principle are energy dependent quantities. However, for the limited energy range of sub-GeV neutrinos, they can be taken to be energy independent and to be close to unity [2,14]. The differential fluxes for electron and muon neutrinos, $d\Phi_e/dE$ and $d\Phi_\mu/dE$, are taken from [8], ν_μ-nucleon CC cross section is taken from [15] and ν_e-nucleon CC cross section is obtained by the approximation $\sigma^{\pi^+}_{e^-}(E) \simeq \sigma^{\pi^+}_{\mu^-}(E + 100\ MeV)$ [2]. The NC cross sections for neutrino energy range 0.5 GeV - 1.5 GeV were taken from [22,23,15]. The corresponding rates in the absence of oscillations can be obtained by setting the survival probability $P_{\alpha\alpha}$ to unity and transition probabilities $P_{\alpha\beta}$ $(\alpha \neq \beta)$ to zero.

III. EXPERIMENTALLY MEASURABLE QUANTITIES

From the processes listed in Eqs. (6) - (9) we see that a π^0 is produced both in the neutral current process defined in Eq. (6) and in the charged current process defined in Eq. (7). The latter process, in general produces three rings (two from the π^0 decay and one from the charged lepton) whereas the former produces only two rings. As discussed in the introduction, the charged current processes in Eq. (8) and (9) also produce two-ring events. Hence, by choosing only two-ring events we can discriminate against the charged current events of the type given in Eq. (7). However, there is a siginificant probability of about

0.17 when the two photons from the π^0 decay cannot be resolved. If the π^0 produced in $\nu_e N \to e\pi^0 N'$ is not resolved into two photons, then we see two diffuse rings in this process also. Such events can be usually rejected because in general their invariant mass will not be near m_π. However, if the π^0 produced in $\nu_\mu N \to \mu\pi^0 N'$ is unresolved, we have a signal of one diffuse and one sharp ring and this process forms a background to the reaction in Eq. (8). Its effect in all the experimental observables must be properly taken into account. An additional process we take into account is the production of two charged pions via the neutral current process

$$\nu_l N \to \nu_l \ \pi^+\pi^- N. \tag{15}$$

This process produces two sharp rings and mimics the reaction given in equation (9). We take its rate to be about 10% of the rate of reaction in equation (9) [13].

Let us define the following experimentally measurable quantities:

1. N_{DD}: The number of events with two diffuse rings.

2. N_{π^0}: The number of events with two diffuse rings whose invariant mass is in the range 90 MeV - 180 MeV.

3. N_{DS}: The number of events with one diffuse and one sharp ring.

4. N_{SS}: The number of events with two sharp rings.

If the detector were ideal and all the particles can be exactly identified, the relations between experimentally measured quantities and theoretically calculable quantities would be $N_{\pi^0} = N^{NC}$, $N_{DS} = N^{CC}_{e^-\pi^+}$ and $N_{SS} = N^{CC}_{\mu^-\pi^+}$. The charged particles can be identified with good efficiency but the efficiency of identifying π^0 events from N_{DD} is only 0.77. There is a 0.17 probability that the two photons from π^0 decay cannot be resolved and the π^0 appears as a single diffuse ring. Thus the CC events with a π^0 in the final state lead to contributions to N_{DS} and N_{SS}. Hence, the modified relations between the experimental and theoretical quantities are

$$N_{\pi^0} = 0.77 N^{NC} + 0.17 \times 0.4 N^{CC}_{e^-\pi^0}$$
$$N_{DS} = N^{CC}_{e^-\pi^+} + 0.17 N^{CC}_{\mu^-\pi^0}$$
$$N_{SS} = N^{CC}_{\mu^-\pi^+} + N^{NC}_{\pi^+\pi^-}. \tag{16}$$

In writing the above equations, we added the contribution of $\nu_\mu N \to \mu^- \pi^0 N'$ to N_{DS} due to the 17% π^0 misidentification probability and the small contribution to N_{SS} due to two charged pion production. We also took into account the contribution of $\nu_e N \to e^- \pi^0 N'$ to N_{π^0} due to the 17% π^0 misidentification probability. Assuming that the directions of the electron and the misidentified π^0 are randomly distributed, we estimate that only about 40% of these events survive the cut on the invariant mass of the two diffuse rings. Hence the factor 0.4 in the correction to the expression for N_{π^0}.

From the experimentally measurable quantities, we define the following three ratios

$$R_1 = \frac{N_{DS}}{N_{\pi^0}}, \tag{17}$$
$$R_2 = \frac{N_{SS}}{N_{\pi^0}}, \tag{18}$$
$$R_3 = \frac{N_{DS} + N_{SS}}{N_{\pi^0}}. \tag{19}$$

Presently the data on one pion events in the atmospheric neutrino experiments is very limited and the errors are quite large. However, we will assume that the large statistics of Superkamiokande will enable it to measure all experimental quantities to an accuracy of better than 10%. Turning now to theoretical uncertainties, the single largest source of error occurs in the ratio [22]

$$\frac{\sigma(\nu_\mu p \to \nu_\mu p \pi^0) + \sigma(\nu_\mu n \to \nu_\mu n \pi^0)}{2\sigma(\nu_\mu n \to \mu^- p \pi^0)} = 0.47 \pm 0.06. \tag{20}$$

This, when combined with other errors, leads to a minimum theoretical uncertainty of about 15% in the predictions of R_1 and R_2. Unfortunately, this uncertainty cannot be reduced and will be part of all future predictions. Still, even with this handicap, we find that the ratios R_1 and R_2 can be used to distinguish between different types of neutrino oscillations.

For the atmospheric neutrino oscillations, based on the mass hierarchy assumption and using CP invariance, the three relevant parameters are ϕ, ψ and δ_{31}. We choose the following ranges for the mixing angles:

- $0 \leq \phi \leq 50^o$. This comes from the analysis of the solar neutrino anomaly. For this region of ϕ, there exist allowed values of ω and δ_{21} which can account for the various solar neutrino data [16,17].

- $30 \leq \psi \leq 90^o$. This comes from our analysis of the zenith angle dependent single ring events of Kamiokande data [20] on atmospheric neutrinos.

For definiteness, we fix $\delta_{31} = 0.001\ eV^2$, which is the central value favored by Superkamiokande analysis of the single ring atmospheric data [7,12]. However, the results do not depend on δ_{31} significantly. The reason for this is that we are averaging over the distance in calculating the number of events and the dependence on δ_{31} is lost during this averaging. We will try to explore how useful the ratios R_1 and R_2 are in distinguishing different regions of the mixing angles. We note that without oscillations (i.e., $\phi = 0$ and $\psi = 0$), these ratios have the values $R_1^{no} = 2.6$ and $R_2^{no} = 3.4$. We plot the values of R_1 and R_2 as functions of the mixing angle ψ for different values of ϕ in figures 1 and 2 resectively. From these we note that for large values of mixing angles, R_1 and R_2 differ significantly from their no oscillation values.

Let us consider three particular cases of maximal oscillations:

1. $\nu_\mu \leftrightarrow \nu_e$ oscillations: In this case, $\psi = 90^o$ and $\phi = 45^o$. Since flux of ν_μ is larger than that of ν_e, the total flux of ν_e increases and that of ν_μ decreases. Hence R_1 increases and R_2 decreases. For this case, $R_1 = 3.8$ and $R_2 = 2.5$. Clearly the change in R_1 and R_2 is more than the 15% uncertainty in the theoretical prediction and one can distinguish this case from that of no oscillations.

2. $\nu_\mu \leftrightarrow \nu_\tau$ oscillations: In this case, $\psi = 45^o$ and $\phi = 0^o$. Here, the flux of ν_μ goes down and that of ν_e is unaffected. Hence R_1 does not change and R_2 decreases. Numerically

we have, $R_1 = 2.6$ and $R_2 = 1.9$. These numbers are significantly different from those of the previous case as well as that of no oscillations. Hence the 15% theoretical uncertainty is no bar in distinguishing this case.

3. Maximal three flavor oscillations: Here all the three flavours mix maximally with one another. This occurs for $\psi = 45^o$ and $\phi \simeq 35^o$. For this case, $R_1 = 2.6$ and $R_2 = 2.2$. Thus the values of R_1 and R_2 together allow us distinguish it from the no oscillation case as well as the two previous cases.

Finally, let us consider the ratio R_3 which is the sum of R_1 and R_2 because already one can extract a value for it from Kamiokande data. The experimental uncertainty is quite large but we will derive the constraints on the neutrino parameter space from the existing data. From [14], we estimate $R_3 = 4.2 \pm 0.7$. The experimental error is about 16%. To this, we add the 15% theoretical error in quadrature. Thus we have $R_3 = 4.2 \pm 1.0$. Fig. 3 shows the plots of R_3 as functions of the angle ψ for different values of ϕ. We note that the upper limit $R_3 \leq 5.2$ imposes the constraint $\psi \leq 70^o$. Hence pure $\nu_\mu \leftrightarrow \nu_e$ oscillations are disfavoured at 1σ level. Figure 4 shows the allowed region in $\phi - \psi$ plane by the Kamiokande constraint on R_3. Already, with the very limited data available, the ratios of 1-pion events yield useful constraints on the allowed neutrino parameter space.

IV. SUMMARY AND DISCUSSION

The atmospheric neutrino experiments have already given us valuable information on the neutrino parameters. So far the bulk of the analysis of the experimental data has been restricted to the single ring events. With the accumulation of more abundant data in the existing and the upcoming detectors, analysis of two-ring events is also likely to be taken up in the future. We have used the framework of the three-flavor oscillations, to suggest such an analysis. We have shown that independent information on the parameters ϕ and ψ can be obtained.

Recently the results of CHOOZ experiment led to strong constraint on the mixing angle $\phi \leq 12.5^o$ [24–26]. This in turn implies that the atmospheric neutrino anomaly is almost due to $\nu_\mu \leftrightarrow \nu_\tau$ oscillations. Current Superkamiokande data on single ring events also favors this explanation. Data on two ring events can provide a dramatic confirmation of this scenario.

Acknowledgements

We thank M. V. N. Murthy, Rahul Sinha, Shashi Kant Dugad and Mohan Narayan for useful conversations. One of us (Balaji) thanks the EHEP, TIFR in Mumbai, and S. S. Rao of IMSc Chennai.

REFERENCES

[1] IMB Collaboration: D. Casper et al., Phys. Rev. Lett. **66**, 2561 (1989); R. Becker-Szendy et al., Phys. Rev **D46**, 3720 (1989).

[2] Kamiokande Collaboration: K. S. Hirata et al., Phys. Lett. **B205**, 416 (1988); *ibid.* **B280**, 146 (1992).

[3] Kamiokande Collaboration: Y. Fukuda et al., Phys. Lett. **B335**, 237 (1994).

[4] Frejus Collaboration: Ch. Berger et al., Phys. Lett. **B227**, 489 (1989); K. Daum et al., Z. Phys. **C66**, 417 (1995).

[5] NUSEX Collaboration: M. Aglietta et al., Europhys. Lett. **8**, 611 (1989).

[6] Soudan 2 Collaboration: M. Goodman et al., Nucl. Phys. **B** (Proc. Suppl.) **38**, 337 (1995); W. W. M. Allison et al., Phys. Lett. **B391**, 491 (1997).

[7] Super-Kamiokande Collaboration: Y. Totsuka, talk at the Lepton-Photon '97, August 1997, Hamburg, Germany; E. Kearns, talk at TAUP 97, LNGS, Assergi, Italy, September 1997.

[8] M. Honda, T. Kajita, K. Kasahara and S. Midorikawa, Phys. Rev. **D52**, 4985 (1995).

[9] V. Agrawal, T. K. Gaiser, Paolo Lipari and Todor Stanev, Phys. Rev. **D53**, 1314 (1996).

[10] V. Barger, K. Whisnant, S. Pakvasa and J. N. N. Phillips, Phys. Rev. **D22**, 2718 (1980).

[11] G. V. Dass and K. V. L. Sarma, Phys. Rev. **D30**, 80 (1984).

[12] M. Gonzalez-Garcia *et al*, LANL archive preprints: hep-ph/9712238, hep-ph/9801368.

[13] F. Vissani and A. Yu. Smirnov, Neutral-to-charged current events ratio in atmospheric neutrinos and neutrino oscillations, hep-ph/9710565.

[14] Kamiokande Collaboration: Y. Fukuda et al., Phys. Lett. **B388**, 397 (1996).

[15] M. Takita, University of Tokyo Thesis, ICR-Report-186-89-3.

[16] M. Narayan, M. V. N. Murthy, G. Rajasekaran and S. Uma Sankar, Phys. Rev. **D53**, 2809 (1996).

[17] G. L.Fogli, E. Lisi and D. Montanino, Phys. Rev. **D53**, 4421 (1996).

[18] J. Pantaleone, Phys. Rev. **D49**, R2152, (1994).

[19] G. L. Fogli, E. Lisi, D. Montanino and G. Scoscia, Phys. Rev. **D55**, 4385 (1997).

[20] M. Narayan, G. Rajasekaran and S. Uma Sankar, Phys. Rev. **D56**, 437 (1997).

[21] N. Hata and P. Langacker, Phys. Rev. **D56**, 6107 (1997).

[22] H. Faissner *et al*, Phys. Lett.. **68B**, 377 (1977).

[23] W. Lee *et al*, Phys. Rev. Lett. **38**, 202 (1977).

[24] M. Apollonio *et al*, Initial Results from the CHOOZ Long Baseline Reactor Neutrino Oscillation Experiment, hep-ex/9711002.

[25] M. Narayan, G. Rajasekaran and S. Uma Sankar, Three flavor implications of CHOOZ result, hep-ph/9712409.

[26] S. M. Bilenky and C. Giunti, Implications of CHOOZ result for decoupling of solar and atmospheric neutrino oscillations, hep-ph/9802201.

FIGURES

FIG. 1. Plot of R_1 vs ψ for $\delta_{31} = 0.001\ eV^2$ and $\phi = 0$ (continuous line), $\phi = 30^0$ (dotted line) and $\phi = 45^o$ (dashed line).

FIG. 2. Plot of R_2 vs ψ for $\delta_{31} = 0.001\ eV^2$ and $\phi = 0$ (continuous line), $\phi = 30^0$ (dotted line) and $\phi = 45^o$ (dashed line).

FIG. 3. Plot of R_3 vs ψ for $\delta_{31} = 0.001\ eV^2$ and $\phi = 0$ (continuous line), $\phi = 30^0$ (dotted line) and $\phi = 45^o$ (dashed line).

FIG. 4. Region in $\phi - \psi$ plane allowed by the Kamiokande constraint on R_3.

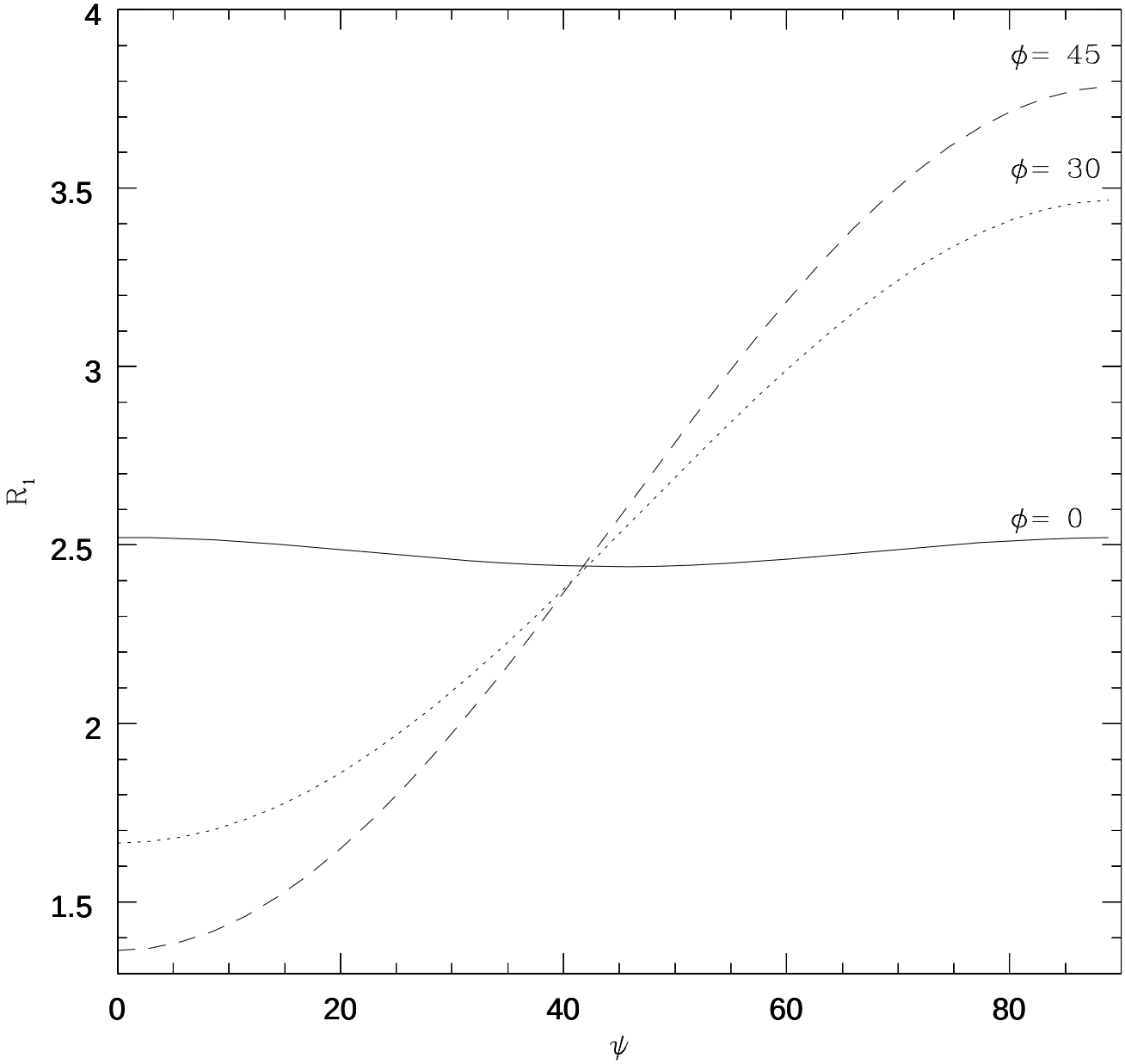

Figure 1

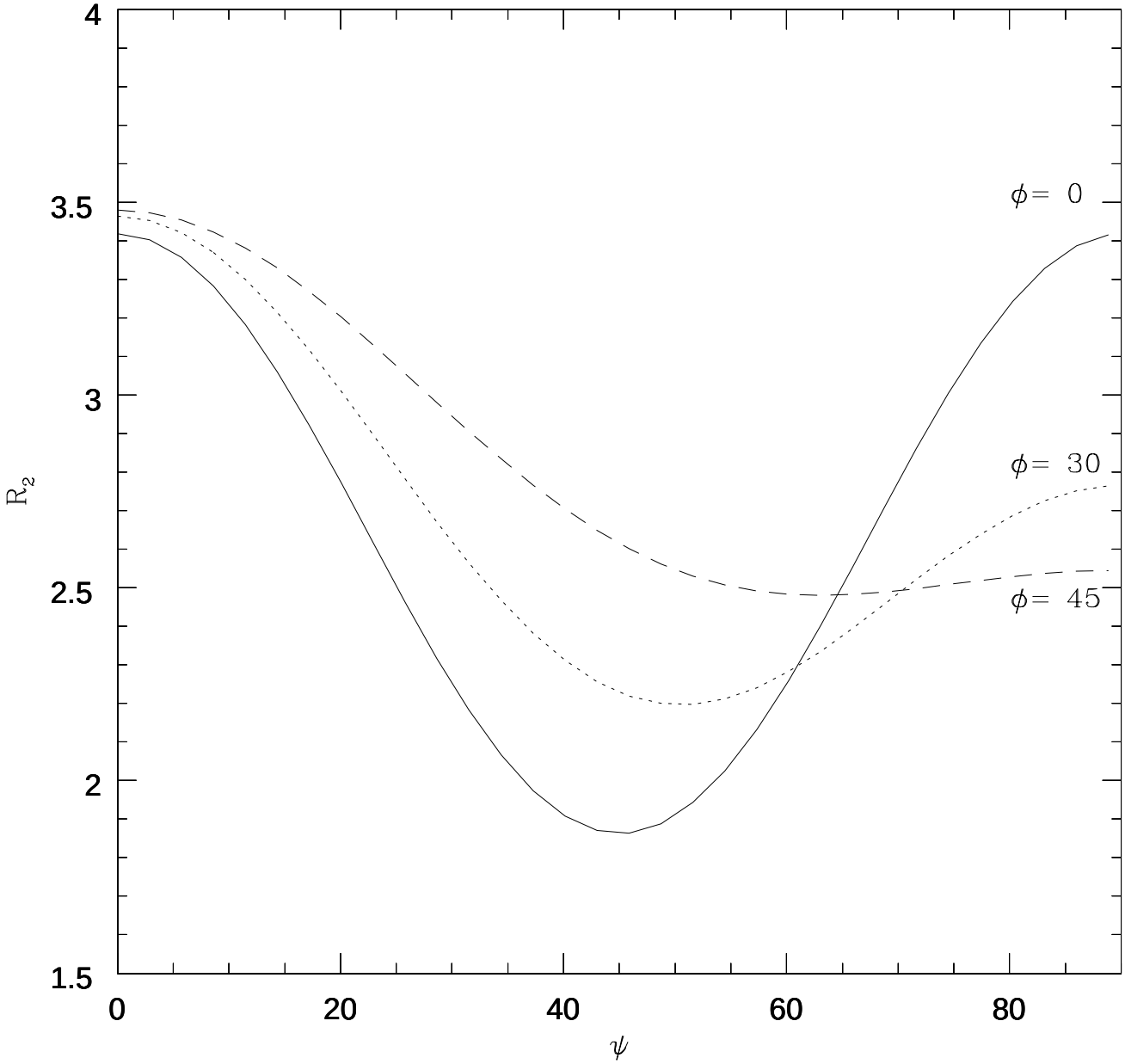

Figure 2

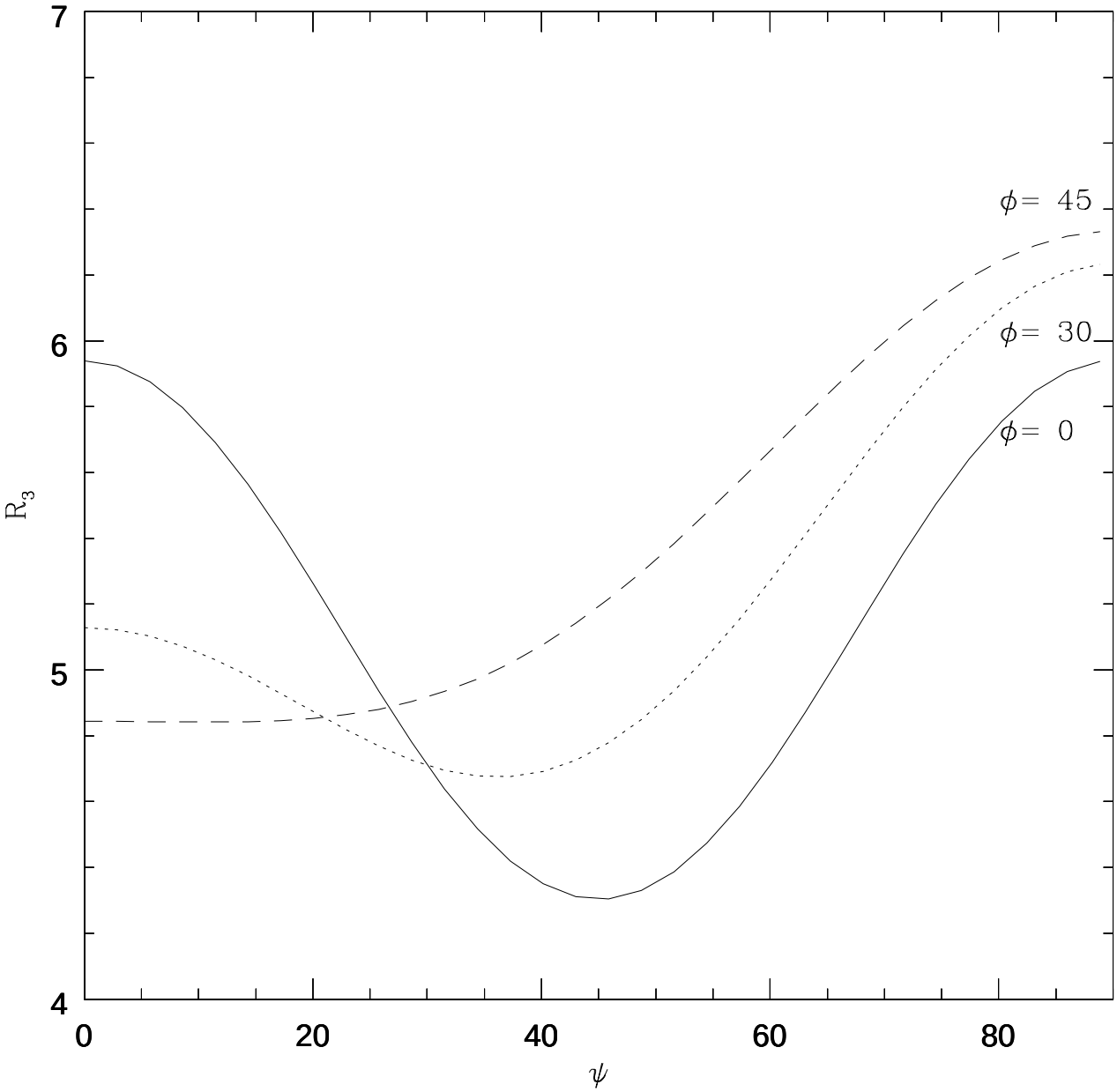

Figure 3

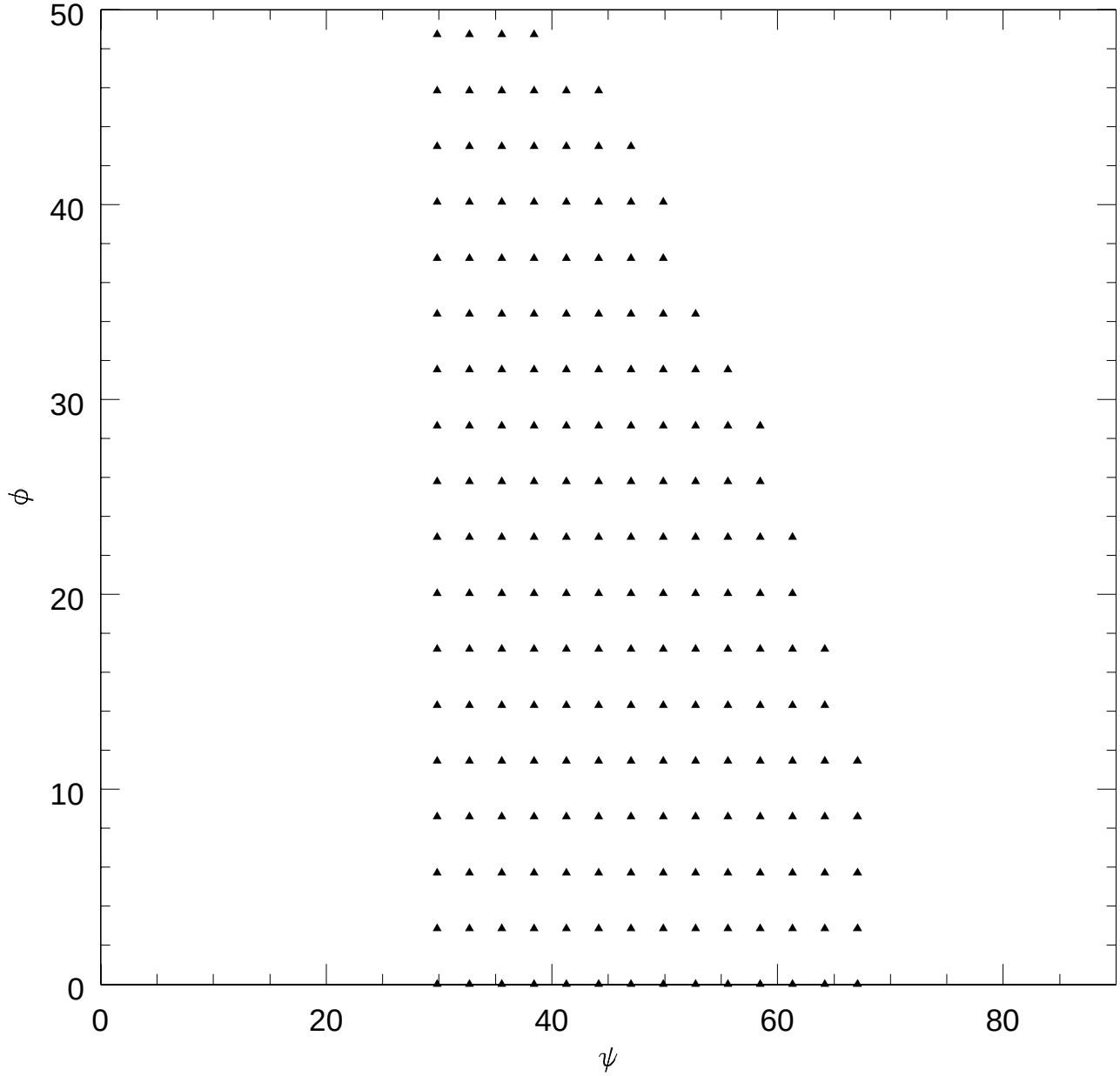

Figure 4